

## $^{17}\text{O}$ Quadrupole Coupling and Chemical Shielding Tensors in an H-bonded Carboxyl Group: $\alpha$ -Oxalic Acid

Qianwen Zhang,<sup>†</sup> Eduard Y. Chekmenev, and Richard J. Wittebort\*

Contribution from the Department of Chemistry, 2320 South Brook Street,  
University of Louisville, Louisville, Kentucky 40292

Received February 4, 2003; E-mail: rjwitt01@athena.louisville.edu

**Abstract:** We have used single crystal  $^{17}\text{O}$  NMR and density functional theory to investigate intermolecular interactions in a strongly H-bonded system. The chemical shielding (CS) and quadrupole coupling (QC) tensors are determined in oxalic acid dihydrate by single crystal methods. With cross polarization from abundant protons, high quality spectra are obtained in 1–2 min from 10  $\mu\text{mol}$  samples. In the crystal lattice, oxalic acid is H-bonded directly to the hydrate with each carboxyl group accepting two H-bonds at C=O and donating one H-bond from COH. The effects of these intermolecular interactions on the experimentally determined QC and CS tensors are modeled by density functional theory with a procedure that accurately calculates, without scaling, the known QC tensors in both gas-phase water and ice. The ice calculation uses a cluster containing 42 waters (in excess of two complete hydration shells). The same procedure applied to a similarly constructed cluster of hydrated oxalic acid gives QC and CS tensors that are within 3–6% of the observed values while isolated molecule tensors are significantly different. Comparison of the isolated molecule tensors with those from either experiment or the cluster calculation shows the magnitude and directionality of intermolecular interactions on the tensors. The isotropic shift of the COH oxygen is deshielded by 29 ppm, and C=O is shielded by 62 ppm while the spans of the CS tensors are increased by 78 ppm and decreased by 73 ppm, respectively. Magnitudes of the quadrupole coupling constants, which are proportional to the electric field gradients at the  $^{17}\text{O}$  sites, decrease by 2.2 and 1.2 MHz at COH and C=O, respectively.

### Introduction

Intermolecular interactions and H-bonding in particular are central to molecular structure and function. NMR spectroscopy is well adapted to investigating H-bonds by correlating, for example, H-bonding with isotropic chemical shifts. Recently, the observation of scalar couplings between H-bonded groups was interpreted as demonstrating the covalent nature of the interaction.<sup>1,2</sup> Although oxygen is often a direct participant in H-bonding,  $^{17}\text{O}$  NMR is infrequently used due to efficient relaxation (wide lines) resulting from a large quadrupole coupling modulated by rotational diffusion. In the solid state, rotational diffusion is absent, resolution is dramatically improved, and the tensor properties of both the quadrupole coupling (QC) and chemical shielding (CS) are observed directly in the resonance frequencies. Since the range of  $^{17}\text{O}$  chemical shifts is large, it is a sensitive monitor of H-bonding as is the quadrupole coupling which is proportional to the electric field gradients from surrounding charges (nuclei and electrons) at the site of the  $^{17}\text{O}$  nucleus.<sup>3–6</sup> Thus, while X-ray and neutron crystallography determine the effects of H-bonding on atomic

positions, the approach used here is more directly related to the effect on electronic structure. Herein we report an experimental determination and density functional theory (DFT) analysis of the QC and CS tensors for the carboxyl group in  $\alpha$ -oxalic acid dihydrate. It contains both H-bond acceptor (C=O) and donor (COH). Principal components and directions for both tensors are determined from indexed single crystals<sup>7–9</sup> (~3 mg) which give spectra with excellent signal:noise (25:1) in 1 or 2 min at 20% enrichment. The QC and CS tensors at the two sites are substantially different. For example, their isotropic shifts are 301 ppm (C=O) and 183 ppm (COH) with an average in good agreement with the exchange averaged signal (250 ppm) observed in solution. The CS principal components for the C=O site span 461 ppm and are more closely related to those reported for a similarly H-bonded amide C=O group (benzamide)<sup>5</sup> than to those determined in benzophenone<sup>5</sup> which lacks H-bond donors. Prior to this report, ice,<sup>8</sup> benzophenone,<sup>7</sup> and the hydrate water of oxalic acid<sup>9</sup> are the only other complete determinations of  $^{17}\text{O}$  tensors by single crystal methods. QC principal compo-

<sup>†</sup> Current address: Tecmag Corp., 6006 Bellaire Blvd., Houston, TX 77081.

- (1) Dingley, A. J.; Grzesiek, S. *J. Am. Chem. Soc.* **1998**, *120*, 8293–8297.
- (2) Comilescu, G.; Hu, J. S.; Bax, A. *J. Am. Chem. Soc.* **1999**, *121*, 2949–2950.
- (3) Wu, G. *Biochem. Cell Biol.* **1998**, *76*, 429–442.
- (4) Dong, S.; Yamada, K.; Wu, G. *Z. Naturforsch. A: Phys. Sci.* **2000**, *55*, 21–28.

(5) Wu, G.; Yamada, K.; Dong, S.; Grondey, H. *J. Am. Chem. Soc.* **2000**, *122*, 4215–4216.

(6) Yamada, K.; Dong, S.; Wu, G. *J. Am. Chem. Soc.* **2000**, *122*, 11602–11609.

(7) Scheubel, W.; Zimmermann, H.; Haerberlen, U. *J. Magn. Reson.* **1985**, *63*, 544–555.

(8) Spiess, H. W.; Garnett, B. B.; Sheline, R. H.; Rabideau, S. W. **1969**, *51*, 1201–1205.

(9) Zhang, Q. W.; Zhang, H. M.; Usha, M. G.; Wittebort, R. J. *Solid State Nucl. Magn. Reson.* **1996**, *7*, 147–154.

nents for a series of carboxylic acids obtained by  $^{17}\text{O}$  NQR have also been reported.<sup>10,11</sup>

To assess the effects of intermolecular interactions such as H-bonding, we compare experiment with density functional theory (DFT). A persistent problem in such calculations is that QC tensor magnitudes are usually overestimated, especially with a small basis set. To account for the level of theory and limited basis set, theoretical values are frequently scaled to improve agreement with experiment.<sup>12</sup> This may, however, lead one to mask the effects of intermolecular interactions which also typically decrease QC tensor component magnitudes (*vide infra*). To establish a useful level of theory and cluster size for modeling intermolecular interactions, we first test the DFT calculations against the experimental values for water, the only case for which both gas-phase<sup>13</sup> and solid-state (ice) QC tensors<sup>8</sup> are known. DFT calculations<sup>14,15</sup> for an isolated molecule using the B3LYP functional and a large basis set (aug-cc-pVDZ) are within experimental error equivalent to the gas-phase QC principal components determined by microwave spectroscopy. Using this basis set and a large cluster<sup>16</sup> containing 42 water molecules, calculated values are also in good agreement with the solid-state NMR QC principal components of ice with no scaling. Theoretical QC and CS principal components at the same level and on a similarly constructed cluster of oxalic acid and water molecules also show good agreement with experiment. This cluster is constructed using neutron structure coordinates<sup>17</sup> and contains 11 oxalic acid and 29 water molecules. On average, QC principal components are overestimated by 3% (0.24 MHz) and CS components by 4% (18 ppm). Tensor orientations are qualitatively correct but agreement is less satisfactory than principal components. Compared to differences between cluster calculation and experiment, differences between the single molecule and cluster calculations are large indicating that intermolecular interactions are modeled at a level sufficient to discuss the size and directionality of H-bonding effects on the tensor components. For example, on comparing a cluster with a single molecule, COH is shifted downfield (deshielded) by 29 ppm, while C=O shifts upfield by 62 ppm. Also the orientations of the largest and intermediate components are interchanged in a way consistent with experiment. The relative importance of using the large cluster is examined in a “core” cluster in which oxalic acid is surrounded only by its directly H-bonded neighbors: four donor and two acceptor waters. To examine indirect H-bond effects, previously reported in a theoretical analysis of  $^{15}\text{N}$  isotropic shifts,<sup>18</sup> either the donor or acceptor waters are eliminated and we find that H-bonding to COH affects the C=O parameters and *vice versa*.

## Methods

**Sample Preparation.** Rectangular plate shaped crystals (2–3 mg) were selected from crystals that grew upon cooling a solution of 40

mg of oxalic acid dihydrate in 250  $\mu\text{L}$  of 20%  $^{17}\text{O}$ -enriched water initially at 50  $^{\circ}\text{C}$ . The  $^{17}\text{O}$  solution NMR spectrum in  $\text{CDCl}_3$  confirmed  $^{17}\text{O}$  exchange labeling at both hydrate (0 ppm, integral = 1) and carboxylate (250 ppm, integral = 2) positions. The space group, lattice dimensions, and crystal morphology were determined by X-ray crystallography and found to be  $P2_1/n$  with  $a = 6.115 \text{ \AA}$ ,  $b = 3.605 \text{ \AA}$ ,  $c = 12.057 \text{ \AA}$ , and  $\beta = 106.2^{\circ}$ , which are equivalent to those for the  $\alpha$  form of oxalic acid.<sup>17</sup> The  $a^*$ -axis is normal to the major morphological plane, and  $b$  is along the longest edge.

**$^{17}\text{O}$  NMR Measurements.** Solid-state  $^{17}\text{O}$  central transition spectra were excited by single<sup>19</sup> and two-level<sup>9</sup> cross polarization with 2–4 ms mixing times and detected with high power  $^1\text{H}$  decoupling using home-built 5.9 and 11.7 T instruments and double resonance goniometer probes.<sup>20</sup>

**Data Analysis.** The procedure used here for obtaining QC,  $\chi$ , and chemical shielding,  $\sigma$ , tensors from the experimental spectra is based on a procedure previously described.<sup>9</sup> In these experiments, the observed central transition frequencies are affected in first order by chemical shielding and in second order by quadrupole coupling. Consequently, observed line frequencies are given by the sum of two frequencies,  $\nu_{\text{CS}}$  and  $\nu_{\text{QC}}$ . With both tensors in a general orientation in a frame with  $z$  along  $\mathbf{B}_0$  and  $y$  along the goniometer rotation axis, the CS contribution to the observed frequency depends only on the tensor component along the field,

$$\nu_{\text{CS}} = -\sigma_{zz}\nu_0 \quad (1)$$

while the  $^{17}\text{O}$  central transition frequency depends on products involving all components of the symmetric, traceless QC tensor,<sup>7</sup>

$$\nu_{\text{QC}} = \frac{1}{1600\nu_0} [8(\chi_{xx} - \chi_{yy})^2 + 32\chi_{xy}^2 - 64(\chi_{xz}^2 + \chi_{yz}^2)] \quad (2)$$

In eq 2, we have used the usual definition of the quadrupole coupling tensor,  $\chi_{ij} = e^2Qq_{ij}/h$ , in terms of electric field gradients,  $q_{ij}$ , and the nuclear quadrupole moment,  $Q$ . To account for sample rotation in the goniometer, both tensors ( $T = \sigma$  or  $\chi$ ) are transformed according to

$$T(\phi) = R_y^T T R_y \text{ with } R_y = \begin{pmatrix} \cos \phi & 0 & -\sin \phi \\ 0 & 1 & 0 \\ \sin \phi & 0 & \cos \phi \end{pmatrix} \quad (3)$$

Substitution of eq 3 into eqs 1 and 2 yields (after some algebra) the following expression for the angular dependence of the frequency for rotation about the  $y$ -axis:

$$\nu_{\text{obs}}^y(\phi) = C_1^y + C_2^y \cos(2\phi) + C_3^y \sin(2\phi) + C_4^y \cos(4\phi) + C_5^y \sin(4\phi) \quad (4)$$

with

$$C_1^y = -28(\tilde{\chi}_{xx}^2 + \tilde{\chi}_{xz}^2 + \tilde{\chi}_{xx}\tilde{\chi}_{yy}) - 16(\tilde{\chi}_{xy}^2 + \tilde{\chi}_{yz}^2) + 11\tilde{\chi}_{yy}^2 + (\tilde{\sigma}_{xx} + \tilde{\sigma}_{zz})/2$$

$$C_2^y = -12\tilde{\chi}_{yy}^2 + 48(\tilde{\chi}_{xy}^2 - \tilde{\chi}_{yz}^2) - 24\tilde{\chi}_{xx}\tilde{\chi}_{yy} + (\tilde{\sigma}_{zz} - \tilde{\sigma}_{xx})/2$$

$$C_3^y = -24\tilde{\chi}_{xz}\tilde{\chi}_{yy} + 96\tilde{\chi}_{xy}\tilde{\chi}_{yz} + \tilde{\sigma}_{xz} \quad (5)$$

$$C_4^y = 36(\tilde{\chi}_{xx}^2 - \tilde{\chi}_{xz}^2 + \tilde{\chi}_{xx}\tilde{\chi}_{yy}) + 9\tilde{\chi}_{yy}^2$$

$$C_5^y = 36\tilde{\chi}_{xz}(2\tilde{\chi}_{xx} + \tilde{\chi}_{yy})$$

and  $\tilde{\chi}_{ij} = \chi_{ij}/1600\nu_0$ ,  $\tilde{\sigma}_{ij} = \sigma_{ij}\nu_0$ . Expressions for rotation about

- (10) Suhara, M.; Smith, J. A. S. *J. Magn. Reson.* **1982**, *50*, 237–248.
- (11) Brosnan, S. G. P.; Edmonds, D. T.; Poplett, I. J. F. *J. Magn. Reson.* **1981**, *45*, 451–460.
- (12) Torrent, M.; Musaev, D. G.; Morokuma, K.; Ke, S. C.; Warncke, K. J. *Phys. Chem. B* **1999**, *103*, 8618–8627.
- (13) Verhoeven, J.; Dymanus, A.; Blyssen, H. *J. Chem. Phys.* **1969**, *50*, 3330–3338.
- (14) Ditchfield, R. *Mol. Phys.* **1974**, *27*, 789–807.
- (15) Wolinski, K.; Hinton, J. F.; Pulay, P. *J. Am. Chem. Soc.* **1990**, *112*, 8251–8260.
- (16) Gornostansky, S. D.; Kern, C. W. *J. Chem. Phys.* **1971**, *55*, 3253–3259.
- (17) Sabine, T. M.; Cox, G. W.; Craven, B. M. *Acta Crystallogr. Sect. B* **1969**, *B25*, 2437–2441.
- (18) Xu, X. P.; Case, D. A. *Biopolymers* **2002**, *65*, 408–423.

- (19) Walter, T. H.; Turner, G. L.; Oldfield, E. *J. Magn. Reson.* **1988**, *76*, 106–120.

- (20) Zhang, Q. W.; Zhang, H.; Lakshmi, K. V.; Lee, D. K.; Bradley, C. H.; Wittebort, R. J. *J. Magn. Reson.* **1998**, *132*, 167–171.

orthogonal axes are obtained by coordinate permutations. The three rotations used here are about the crystal  $b$ -axis ( $x = -c, y = b, z = a^*$ ), about the  $c$ -axis rotation ( $x = b, y = c, z = a^*$ ), and about the  $a^*$  axis ( $x = -c, y = a^*, z = -b$ ). The 15 constants,  $C_j^k$ , are determined by linear least-squares fitting of the experimental line frequencies and constitute the basic data from which the 11 unique elements of the QC and CS tensors are determined. For purposes of evaluating experimental errors, tensors were determined at 5.9 T ( $\nu_0 = 34.25$  MHz) and at 11.7 T ( $\nu_0 = 67.15$  MHz) to take advantage of the field dependence of the two interactions. Doubling  $B_0$ , for example, doubles the chemical shift and halves the quadrupole contributions to the observed frequencies.

Two approaches, based on a Newton–Raphson algorithm,<sup>7</sup> were used to solve eq 5, a system of nonlinear equations. In the first “single field” method, an arbitrary combination of 11 equations is chosen from the above set and solved for the 11 tensor components. In practice, eight solutions are found, and extraneous solutions are eliminated by using different combinations of the equations to find the common set of parameters. In the second “combined field” approach, the shielding and quadrupole contributions to the coefficients  $C = C_1^k, C_2^k$ , and  $C_3^k$  were separated using their known magnetic field dependence:

$$\begin{aligned} C^{5.9\text{T}} &= C_{\text{CS}}^{11.7\text{T}}/r + C_{\text{QC}}^{5.9\text{T}} \\ C^{11.7\text{T}} &= C_{\text{CS}}^{11.7\text{T}} + C_{\text{QC}}^{5.9\text{T}}/r \end{aligned} \quad (6)$$

where,  $r = 11.7$  T/5.9 T. This results in 9 linear equations for the 6 shielding components and 15 nonlinear equations for the 5 electric field gradient components. QC and CS tensors obtained using the “single field” approach at both spectrometer frequencies and the “combined field” approach are in good agreement. Given the high signal-to-noise ratio of the spectra and the narrow lines ( $\sim 200$  Hz), we anticipate that errors in the tensor principal components and orientations are largely systematic resulting from small errors in crystal alignments. Thus, the averages and standard deviations of results from the three determinations described above using two separate crystals are reported. Standard errors reported for the tensor principal components (eigenvalues) and directions (eigenvectors) were determined by propagating the standard errors in the tensor components using Monte Carlo analysis.<sup>21,22</sup>

**Theoretical Calculations.**  $^{17}\text{O}$  electric field gradient (EFG) and chemical shielding tensors were calculated using the Gaussian98<sup>23</sup> program. The computations reported here for isolated molecules and small clusters use density functional theory (DFT), the B3LYP functional, and the Dunning correlation consistent double- $\zeta$  basis set (aug-cc-pVDZ) which contains both diffuse and polarization functions.<sup>24</sup> In some cases, as noted, we have eliminated the diffuse functions or used a locally dense approach with a smaller basis set, 3-21g\*, on all molecules except those of the core cluster, the molecule of interest and its directly H-bonded neighbors. Clusters were constructed using neutron coordinates and, as previously suggested for the calculation of quadrupole couplings,<sup>12</sup> DFT calculations were performed without geometry optimization. EFG tensor components in atomic units,  $q_{ij}$ ,

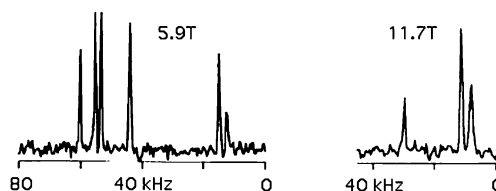


**Figure 1.** Single crystal  $^{17}\text{O}$  NMR spectra of  $\alpha$ -oxalic acid dihydrate. The spectrum obtained at 5.9 T (256 transients) is recorded from the  $a^*$ -axis rotation at a goniometer setting of  $\phi = 155^\circ$  and the 11.7 T spectrum (128 transients) is from the  $b$ -axis rotation with  $\phi = 125^\circ$ .

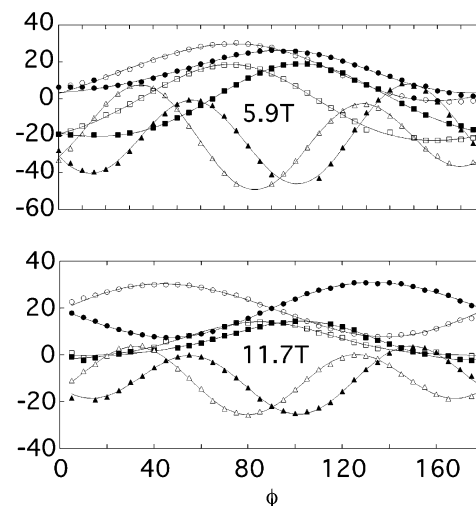


**Figure 2.** Line frequencies as a function of goniometer angle,  $\phi$ , for rotation about the crystallographic  $c$ -axis at two field strengths. The assignments (see text) are  $\text{H}_2^{17}\text{O}$  (triangles),  $\text{C}=\text{C}^{17}\text{O}$  (circles), and  $\text{C}^{17}\text{O H}$  (squares).

are related to the quadrupole coupling tensor components,  $\chi_{ij}$ , by  $\chi_{ij} = e^2q_{ij}Q/h = -2.3496Qq_{ij}$ .<sup>6</sup> We have used the accepted value of the nuclear quadrupole moment  $Q = -2.558$ <sup>25</sup> rather than treating it as an adjustable parameter; that is,  $\chi_{ij} = 6.01q_{ij}$  MHz. For ready comparison with experiment, DFT CS components,  $\sigma_{ij}$ , are reported here as shifts,  $\delta_{ij}$ , relative to water using the absolute  $^{17}\text{O}$  shielding scale established by Wasylshen,  $\delta_{ij} = 307.9 - \sigma_{ij}$ .<sup>26</sup>

## Results

Single crystal cross-polarization spectra at  $B_0 = 5.9$  T and 11.7 T are shown in Figure 1. Spectra with good sensitivity are obtained with 256 (5.9 T) or 128 (11.7 T) transients using a 1 s recycle delay with a 2–3 mg crystal at the 20% enrichment level. For the general orientation, six lines are observed corresponding to the three chemically distinct  $^{17}\text{O}$  sites in two magnetically nonequivalent, symmetry-related molecules. It is expected that this magnetic nonequivalence is lost in the  $b$ -axis rotation, and this is experimentally confirmed (Figure 1).

Line frequencies for the  $c$ -axis rotations at both field strengths are shown in Figure 2. Assignments are based on (i) spectra obtained without high power  $^1\text{H}$  decoupling wherein only the nonprotonated carbonyl oxygen is observed and (ii) the large quadrupole coupling and small shielding anisotropy of the hydrate signal readily seen by comparing the 5.9 T and 11.7 T rotation plots (Figure 2). The observation of three lines for the  $b$ -axis spectra and pairwise crossing of the curves for symmetry-related sites in the  $c$ - and  $a^*$ -axis rotations at  $\phi = 90^\circ$  confirms

(21) Press, W. H.; Flannery, B. P.; Teukolsky, S. A.; Vetterling, W. T.; Chipperfield, J. R. *Numerical recipes: the art of scientific computing*; Cambridge University Press: Cambridge, 1988.

(22) Chekmenev, E. Y.; Xu, R. Z.; Mashuta, M. S.; Wittebort, R. J. *J. Am. Chem. Soc.* **2002**, *124*, 11894–11899.

(23) Frisch, M. J.; Trucks, G. W.; Schlegel, H. B.; Scuseria, G. E.; Robb, M. A.; Cheeseman, J. R.; Zakrzewski, V. G.; Montgomery, J. A., Jr.; Stratmann, R. E.; Burant, J. C.; Dapprich, S.; Millam, J. M.; Daniels, A. D.; Kudin, K. N.; Strain, M. C.; Farkas, O.; Tomasi, J.; Barone, V.; Cossi, M.; Cammi, R.; Mennucci, B.; Pomelli, C.; Adamo, C.; Clifford, S.; Ochterski, J.; Petersson, G. A.; Ayala, P. Y.; Cui, Q.; Morokuma, K.; Malick, D. K.; Rabuck, A. D.; Raghavachari, K.; Foresman, J. B.; Cioslowski, J.; Ortiz, J. V.; Baboul, A. G.; Stefanov, B. B.; Liu, G.; Liashenko, A.; Piskorz, P.; Komaromi, I.; Gomperts, R.; Martin, R. L.; Fox, D. J.; Keith, T.; Al-Laham, M. A.; Peng, C. Y.; Nanayakkara, A.; Gonzalez, C.; Challacombe, M.; Gill, P. M. W.; Johnson, B.; Chen, W.; Wong, M. W.; Andres, J. L.; Gonzalez, C.; Head-Gordon, M.; Replogle, E. S.; Pople, J. A. *Gaussian98*, revision A.7 ed. Gaussian, Inc.: Pittsburgh, PA, 1998.

(24) Woon, D. E.; Dunning, T. H. *J. Chem. Phys.* **1993**, *98*, 1358–1371.

(25) Pyykko, P. Z. *Naturforsch. A: Phys. Sci.* **1992**, *47*, 189–196.

(26) Wasylshen, R. E.; Mooibroek, S.; Macdonald, J. B. *J. Chem. Phys.* **1984**, *81*, 1057–1059.

**Table 1.**  $^{17}\text{O}$  QC Tensors ( $\chi$ ) for  $\alpha$ -Oxalic Acid Dihydrate<sup>a</sup>

	$\chi_{xx}$	$\chi_{yy}$	$\chi_{zz}$	$x$	$y$	$z$
C=O	<b>-3.88(0.19)</b>	<b>-4.49(0.22)</b>	<b>8.30(0.23)</b>	plane	orthog	C=O
$a^*$	0.211(0.234)	0.839(0.059)	0.439(0.006)	-0.523	-0.114	0.847
$b$	0.932(0.068)	-0.242(0.260)	0.015(0.006)	-0.851	0.013	-0.521
$c$	-0.119(0.114)	-0.405(0.037)	0.898(0.006)	0.049	-0.993	-0.104
COH	<b>2.80(0.23)</b>	<b>3.88(0.25)</b>	<b>-6.68(0.08)</b>	plane	orthog	COH
$a^*$	-0.432(0.184)	0.588(0.024)	0.658(0.005)	-0.523	-0.611	-0.594
$b$	0.848(0.058)	0.437(0.235)	0.177(0.008)	-0.851	0.414	0.324
$c$	0.183(0.153)	-0.635(0.069)	0.732(0.005)	0.049	0.675	-0.737

<sup>a</sup> Principal components (MHz) are in bold, and corresponding eigenvectors and reference vectors are in the crystal ( $a^*$ ,  $b$ ,  $c$ ) frame. Reference vectors specify the normal to the OCO plane ( $x$ ), the C=O or C—OH bond ( $z$ ), and the mutually orthogonal direction ( $y$ ). Standard errors are in parentheses.

**Table 2.**  $^{17}\text{O}$  CS Tensors for  $\alpha$ -Oxalic Acid Dihydrate<sup>a</sup>

	$\delta_{11}$	$\delta_{22}$	$\delta_{33}$	$x$	$y$	$z$
C=O	<b>476(18)</b>	<b>413(11)</b>	<b>14(13)</b>	plane	orthog	C=O
$a^*$	-0.844(0.051)	-0.235(0.114)	0.464(0.029)	-0.523	-0.114	0.847
$b$	0.345(0.059)	0.402(0.043)	0.845(0.012)	-0.851	0.013	-0.521
$c$	0.386(0.116)	-0.874(0.063)	0.263(0.016)	0.049	-0.993	-0.104
COH	<b>351(4)</b>	<b>142(3)</b>	<b>55(4)</b>	plane	orthog	COH
$a^*$	-0.480(0.011)	-0.755(0.019)	0.446(0.029)	-0.523	-0.611	-0.594
$b$	0.458(0.010)	0.218(0.035)	0.861(0.009)	-0.851	0.414	0.324
$c$	0.748(0.008)	-0.617(0.014)	-0.241(0.030)	0.049	0.675	-0.737

<sup>a</sup> Principal components,  $\delta_{ij}$ , are in bold and in ppm relative to water. Eigenvectors and orthogonal reference vectors are in the crystal ( $a^*$ ,  $b$ ,  $c$ ) frame. Standard errors are in parentheses.

that the unit cell was correctly oriented relative to the crystal morphology.

Experimentally determined  $^{17}\text{O}$  QC and CS parameters are collected in Tables 1 and 2 which list tensor principal components, corresponding eigenvectors and local reference vectors in the ( $a^*$ ,  $b$ ,  $c$ ) frame. The QC tensor for the hydrate water molecule has been reported previously.<sup>9</sup> Two ambiguities typically encountered in single crystal determinations were resolved to obtain these tensors. Specifically, four symmetric shielding tensors are consistent with the experiment. For CS at the C=O site, they are as follows (components are in ppm with experimental uncertainties in parentheses):

$$\delta_{\pm,\pm} = \begin{pmatrix} 373(20) & \pm 176(10) & -68(2) \\ \cdots & 136(9) & \pm 81(2) \\ \cdots & \cdots & 395(13) \end{pmatrix}$$

Tensors  $\delta_{++}$  and  $\delta_{--}$  (or  $\delta_{+-}$  and  $\delta_{-+}$ ) have the same principal components and correspond to symmetry-related molecules in the unit cell. Two symmetry-related pairs result from the use of rotation axes that are crystal axes (Figure 2). They have different eigenvalues, and only one is correct. Ambiguities are resolved by comparing experiment with DFT calculation. The eigenvalues select the correct pair, and the eigenvectors assign symmetry-related tensors to the correct site in the unit cell. For example, the C= $^{17}\text{O}$  eigenvalues are either 14, 413, and 476 ppm or 38, 330, and 536 ppm, and the DFT values (described below) are 11, 433, and 505 ppm in good agreement only with the first choice. Similarly clear-cut is for C $^{17}\text{OH}$  where experimental eigenvalues are either 13, 230, and 305 ppm or 55, 142, and 351 ppm, and the DFT values are 66, 167, and 349 ppm.

The excellent sensitivity in the  $^{17}\text{O}$  spectra results, in large part, from the use of cross polarization wherein magnetization

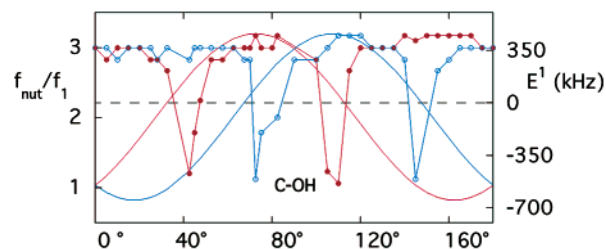


**Figure 3.** Variation of  $f_{\text{nut}}/f_1$  (circles) and the first-order quadrupole energy,  $E^1$  (lines), for the C $^{17}\text{OH}$  signal as a function of crystal orientation. The sample is rotated about the  $a^*$ -axis, and the two colors correspond to symmetry-related sites.

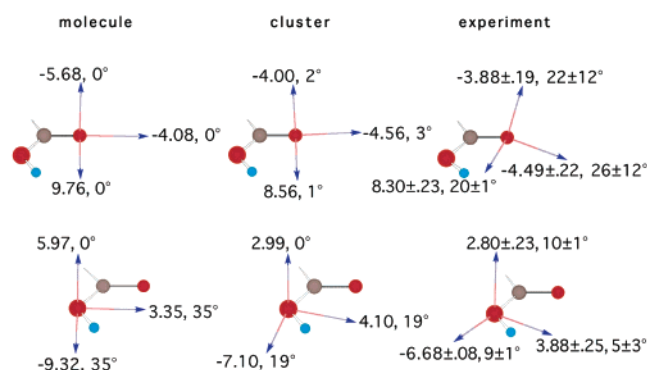


**Figure 4.** Calculated and experimental QC tensor principal components (MHz) for the oxalic acid C $^{17}\text{O}_2\text{H}$  group. Each angle is the difference in orientation between the principal axis and the nearest axis of the reference frame defined in Table 1.

is transferred from  $^1\text{H}$  to  $^{17}\text{O}$  by matching their rotating frame energy levels. These energies are the nutation frequencies of  $^1\text{H}$  and  $^{17}\text{O}$  about their resonant RF fields. For spin  $5/2$  ( $^{17}\text{O}$ ), the nutation frequency is  $f_{\text{nut}}/f_1 = 3$  in the limit of quadrupole coupling large compared to the RF field or  $f_{\text{nut}}/f_1 = 1$  with quadrupolar interaction small compared to the RF field strength,  $f_1$ .<sup>19</sup> In single crystal experiments, the quadrupolar frequencies are systematically varied as the sample is rotated, and the result of this on the Hartman–Hahn match required for observing a C $^{17}\text{OH}$  signal is shown in Figure 3. Also plotted in Figure 3 is the first-order quadrupole energy,<sup>7</sup>  $E^1$ , calculated using the experimentally determined quadrupole tensor, Table 1. The sharp change in nutation frequency from  $f_{\text{nut}}/f_1 = 3$  to  $f_{\text{nut}}/f_1 = 1$  coincides with vanishing  $E^1$  and indicates that the tensor orientations determined here are correct. The angular range over which  $f_{\text{nut}}/f_1 \neq 3$  is observed to be  $\sim 20^\circ$ . We note that the effect of cross-polarization efficiency on line intensities has no effect on the tensor principal components and orientations reported here which are based entirely on line frequencies in single crystal spectra, Figure 2. Previously, QC principal components for  $\alpha$ -oxalic acid obtained from double resonance NQR powder spectra have been reported.<sup>11</sup> While C=O values are in good agreement, their COH QC coupling ( $\chi_{zz} = -7.54$  MHz<sup>11</sup>) is larger than that reported here ( $\chi_{zz} = -6.68$  MHz). Given the indicated uncertainties in interpreting their powder pattern line shapes,<sup>11</sup> we anticipate the results reported here are more reliable.

The tensors of Tables 1 and 2 are pictured relative to the carboxyl group in Figures 4 and 5 (QC and CS, respectively). Also given is the angle between each principal axis and the nearest axis of an orthogonal reference frame ( $x$  normal to the molecular plane and  $z$  along the C—O or C=O vector). For

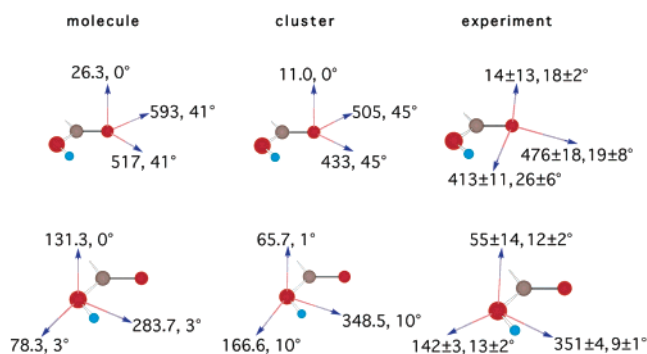


**Figure 5.** Calculated and experimental CSA tensor principal components (ppm). Each angle is the difference in orientation between the principal axis and the nearest axis of the reference frame defined in Table 2.

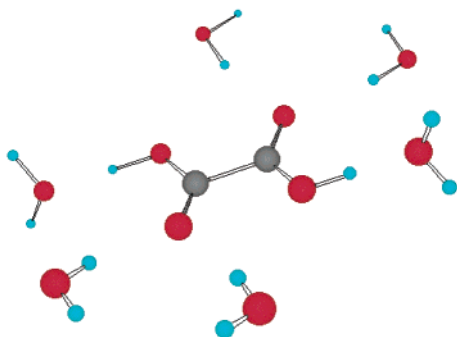


**Figure 6.** Core cluster containing oxalic acid and the six directly H-bonded waters. Coordinates are taken from the neutron structure of  $\alpha$ -oxalic acid.<sup>17</sup>

both COH and C=O, orientations of the QC and CS principal axes are similar, as previously observed for amide C=O groups.<sup>5,6</sup> Uncertainties in orientations are small with the exception of the nearly axially symmetric QC tensor for C=O, where only the large component direction is accurately determined. These orientations are in qualitative agreement with calculations for amide carbonyl oxygens.<sup>5,6</sup> Deviations from orientation along a bond or a molecular plane normal range from 10° to 22°. Both COH and C=O groups have the QC component of smallest magnitude and the most shielded CS component approximately normal to the molecular plane. Components closest to their carbon–oxygen bonds are as follows: the QC component of largest magnitude for COH, the QC component of intermediate magnitude for C=O, the least shielded CS component for C=O, and the intermediate CS component for COH. In terms of interacting most directly with H-bond partners, Figure 6, the  $-4.49$  MHz component approximately along the C=O bond points toward two H-bond donors while the  $+3.88$  MHz principal component of the COH oxygen points toward a single H-bond acceptor. The least shielded components of both C=O (476 ppm) and COH (351 ppm) point approximately toward the H-bond donor and acceptor, respectively. Isotropic chemical shifts of the C=O, 301 ppm, and the COH, 183 ppm, are quite different.

The effects of intermolecular interactions on the  $^{17}\text{O}$  QC tensor have been studied in ice by comparing gas-phase and solid-state experiments. Here, we compare experiment with CSA and QC calculations of isolated molecules and clusters constructed in such a way as to model intermolecular interactions.<sup>3–6,14,27</sup> To select the level of theory and basis, we compare calculation with the known gas-phase QC tensor for water ( $\chi_{zz}$

**Table 3.** Comparison of DFT and Experimental QC Principal Component Values for an Isolated Water (1W) and Clusters (5W, 17W, and 42W) with Gas-Phase and Solid-State Experimental Values, Respectively<sup>a</sup>

system	$\chi_{xx}$	$\chi_{yy}$	$\chi_{zz}$
W(g) exptl <sup>13</sup>	$-1.28(0.09)$	$-8.89(0.03)$	$10.18(0.07)$
1W	$-1.39$	$-8.74$	$10.13$
W(s) exptl <sup>8</sup>	$-0.22(0.1)$	$-6.44(0.1)$	$6.66(0.1)$
5W	$-0.15$	$-7.23$	$7.38$
17W	$-0.06$	$-6.83$	$6.90$
42W	$-0.04$	$-6.69$	$6.73$

<sup>a</sup> The molecular geometries used in the calculations are the experimentally determined bond lengths and valence angles in gas phase<sup>13</sup> (1W) and normal ice (5W, 17W, and 42W). The H-bond distance in the clusters is that determined by neutron diffraction.<sup>30</sup>

$= 10.18 \pm 0.06$  MHz<sup>13</sup>). Previously, the Hartree–Fock theory with the 6-311+g(d,p) basis set was used to successfully calculate the proton shielding anisotropy in ice.<sup>27</sup> We find that with the 6-311+g(2d,p) basis set, DFT ( $\chi_{zz} = 10.76$  MHz) is improved over the Hartree–Fock result ( $\chi_{zz} = 11.11$  MHz). With a larger basis set, aug-cc-pVDZ, the Hartree–Fock calculation is comparable to DFT with 6-311+g(2d,p) and the DFT calculation converges to the experimental values (Table 3) essentially within experimental errors (0.03 to 0.09 MHz) or the anticipated effects from vibrational averaging (0.05 to 0.22 MHz).<sup>28</sup> To determine the cluster size, we compare ice QC values<sup>8</sup> with clusters containing 5, 17, and 42 waters. While a five water (5W) cluster contains the first hydration sphere with all directly H-bonded groups, it was suggested that a correct model of H-bonding in ice requires a cluster of 17 waters (17W) which contains three molecules H-bonded to each of the outer molecules of the first sphere.<sup>15,27</sup> The surface of this cluster is irregular, and the addition of 25 waters from the third hydration sphere fills the cavities giving an approximately spherical 42W cluster. At the B3LYP/aug-cc-pVDZ level, agreement improves with cluster size and the 42W calculation is in substantial agreement with experiment (Table 3). Including the first hydration sphere (5W), accounts for 80% of the 3.5 MHz difference between the gas- and solid-phase couplings. The 42W calculation, which used the smaller basis set for atoms in the second and third hydration spheres,<sup>27,29</sup> outperformed the 17W calculation and required half the computational time.

Consequently, this approach and the known crystal packing<sup>17</sup> were used to construct the cluster for oxalic acid hydrate calculations. The core H-bonded cluster (aug-cc-pVDZ basis set) contains one oxalic acid molecule with six directly H-bonded waters (Figure 6). The calculation includes an additional 10 oxalic acid and 23 water molecules (3-21g\* basis set) H-bonded either to or in close contact with core molecules. Coordinates for this cluster and the 42W cluster are included in the Supporting Information.

Calculated QC and CSA tensors for a single molecule and this cluster are compared with experiment in Figures 4 and 5. The principal values of the DFT QC and CSA tensors for the clusters are in substantial agreement with experiment and distinct from the single molecule values indicating that intermolecular effects are reliably modeled and have a large effect on the  $^{17}\text{O}$  QC and CSA tensors. Typically, magnitudes of the cluster

(27) Hinton, J. F.; Guthrie, P.; Pulay, P.; Wolinski, K. *J. Am. Chem. Soc.* **1992**, *114*, 1604–1605.

(28) Ermler, W. C.; Kern, C. W. *J. Chem. Phys.* **1971**, *55*, 4851.

(29) Chesnut, D. B.; Foley, C. K. *Chem. Phys. Lett.* **1985**, *118*, 316–321.

principal components are larger than experimental values by an amount comparable to the estimated experimental error. Calculated QC constants,  $\chi_{zz}$ , are in error by 3% (C=O) or 6% (COH), and shielding spans,  $\delta_{11} - \delta_{33}$ , by 6% (C=O) or -5% (COH). With the exception of the in-plane components of the C=O CS tensor, orientations are also in reasonable agreement with experiment. A noteworthy feature of the calculations is that orientations of the small and intermediate QC and CS tensor components are interchanged in the single molecule and cluster calculations with those for the latter confirmed by experiment.

In the context of H-bond geometry (Figure 6), we summarize effects of H-bonding on the tensors. C=O accepts two H-bonds symmetrically positioned about the bond axis and in the molecular plane. In qualitative agreement with early Hartree–Fock calculations on a formic acid dimer,<sup>31</sup> the smallest change is a 0.48 MHz increase in the magnitude of the negative component along the bond and the largest change is a 1.68 MHz decrease in the positive component orthogonal to both the molecular plane and the bond. In contrast, the CS component in this direction is least affected (shielded by 15 ppm) with larger upfield shifts (~85 ppm) for both in-plane components. The isotropic chemical shift moves upfield by 63 ppm, and the shielding span is decreased by 73 ppm. For COH, which accepts a single H-bond along the O–H bond and in the molecular plane, the QC and CS principal components are not close to the H-bond direction. Changes in QC components are larger ( $\chi_{zz}$  is reduced by 2.22 MHz) and all components are affected. All shielding components are also affected. Components in the molecular plane are shifted downfield (65 or 88 ppm) while the mutually orthogonal component is shifted upfield (66 ppm). Consequently, the isotropic chemical shift is deshielded by 29 ppm, and the span of the tensor increases by 78 ppm.

<sup>17</sup>O tensor orientations determined relative to the molecular frame have not previously been compared with DFT calculations. Agreement is satisfactory for COH but less so for C=O where typical errors are ~20°. The worst case is the C=O CS tensor (in-plane components), and the best case is the COH CS tensor. In all cases, differences in orientation between the single molecule and cluster calculation are small.

## Discussion

Reported here are complete QC and CS tensor determinations for the oxygens in a carboxyl group. DFT calculations of the QC and CS principal components for clusters at the B3LYP/aug-cc-pVDZ level are in good agreement with experiment. Correlation of theory with experiment gives slopes of 1.04 for the QC components or 1.03 for the CS components without scaling (correlation coefficients are 0.999 and 0.998) and thus compare well with the ideal slope of unity. Consequently, tensor components were not empirically scaled down, and intermolecular effects, which also typically decrease tensor component magnitudes, are less likely to be masked. Combined with accurate theory, the solid-state <sup>17</sup>O NMR experiment is a sensitive and direct probe of H-bonding.

With large molecules, large basis sets and clusters are a potential impediment. Compared to those used here, smaller

**Table 4.** Effect of Basis Set and Cluster Size on  $\chi_{zz}$  and  $\delta_{11}$  in Water/Oxalic Acid Clusters<sup>a</sup>

cluster	diffuse functions	$\chi_{zz}$ (COH)	$\delta_{11}$ (COH)	$\chi_{zz}$ (C=O)	$\delta_{11}$ (C=O)
OA	yes	-9.32	283.7	9.76	593
2W	yes	-7.62	308.3	9.63	576.1
4W	yes	-9.02	302.6	8.86	536.5
6W	no	-7.78	329.9	8.76	508.4
6W	yes	-7.42	330.1	8.64	515.4
29W	yes	-7.10	348.5	8.56	505.3
exptl	- - -	-6.68	350	8.30	475

<sup>a</sup> The 6W cluster is that shown in Figure 6. The 2 waters H-bonded to the COH groups are removed in 4W while the 4 waters H-bonded to the C=O groups are removed in 2W. 29W is that used for the calculations in Figures 4 and 5.

basis sets and cluster sizes have been previously used for interpretation of experiments with larger molecules. For example, amide carbonyl principal components have been compared with DFT calculations using the same functional, somewhat smaller basis set, D95\*\*, and dimers or trimers.<sup>4–6</sup> In this work, the slope of the theory versus experiment correlation was 1.125 for shielding, and the nuclear quadrupole moment was scaled to 91% of the accepted value.<sup>6</sup> By systematically stripping down our calculations (Table 4), we can examine what features are important. Note that the test case for the computational protocol used here is QC in water, which, unlike the two oxygen sites in oxalic acid, is both an H-bond acceptor and donor. Including diffuse functions is helpful for improving the electric field gradient calculation but makes little or no improvement in shielding. Furthermore, the large cluster is primarily important for a reasonable description of the COH tensors while H-bonding effects are more localized in the core cluster for the calculation of the C=O tensors. Effects of H-bonding to the oxygen of interest (direct) or H-bonding to a neighboring oxygen in the same molecule (indirect) are examined by further stripping to the 4W or 2W clusters. Direct and indirect effects on shielding are similar (20–25 ppm) with the exception of the direct H-bond at C=O which is twice as large (57 ppm). A substantial indirect effect has been previously reported in DFT calculations of <sup>15</sup>N amide isotropic shifts where H-bonding to the attached carbonyl results in a larger shift than the direct amide H-bond shift.<sup>18</sup> We conclude by noting that analysis of QC in H-bond donors appears to require large clusters and basis sets while chemical shielding in H-bond acceptor oxygens is more tractable.

An experimental impediment to the use of <sup>17</sup>O NMR in biomolecules and polymers is poor sensitivity. In the work reported here, high quality spectra (S:N > 25:1) are obtained from small samples (10  $\mu$ mol of <sup>17</sup>O per site) in short periods of time (~2 min). This is a result of the anticipated ~8-fold sensitivity increase from cross polarization relative to direct <sup>17</sup>O excitation. Typically, however, single crystals are not available, and magic angle spinning of randomly oriented samples is used with direct excitation<sup>2–6</sup> to avoid deleterious effects of MAS on cross polarization with a quadrupolar nucleus. Irradiation schemes to overcome this problem have been described<sup>32</sup> but not demonstrated in the context of <sup>17</sup>O NMR. Another approach described some time ago<sup>33</sup> renders the first-order quadrupole coupling time independent by switching the spinning axis onto

(30) Eisenberg, D.; Kauzman, W. *The Structure and Properties of Water*; Oxford University Press: 1969.

(31) Gready, J. E. *Chem. Phys.* **1981**, *55*, 1–26.

(32) Rovnyak, D.; Baldus, M.; Griffin, R. G. *J. Magn. Reson.* **2000**, *142*, 145–152.

(33) Gann, S. L.; Baltisberger, J. H.; Wooten, E. W.; Zimmermann, H.; Pines, A. *Bull. Magn. Reson.* **1994**, *16*, 68.

the static field for cross polarization and subsequently off-axis for detection. Figure 3 confirms that the first-order quadrupole coupling alone is sufficient to describe the quadrupole interaction during cross polarization. Revisiting this approach should be an attractive avenue to pursue  $^{17}\text{O}$  NMR in more complicated molecules.

**Acknowledgment.** We wish to thank Professors Pawel Kozlowski and Gene Lamm for helpful suggestions on the

computational aspects of this work and critically reading the manuscript and Gene Lamm for maintaining the Linux cluster.

**Supporting Information Available:** Included are tables of coordinates for the 29W oxalic acid and the 42W ice cluster. This material is available free of charge via the Internet at <http://pubs.acs.org>.

JA034495E